Author Manuscript

Author Manuscript

Author Manuscript

Author Manuscript

HHS Public Access

Author manuscript

Exp Eye Res. Author manuscript; available in PMC 2024 November 01.

Published in final edited form as:

Exp Eye Res. 2023 November ; 236: 109675. doi:10.1016/j.exer.2023.109675.

Differential expression of PIEZO1 and PIEZO2 mechanosensitive channels in ocular tissues implicates diverse functional roles

Ying Zhu[1], **Julian Garcia-Sanchez**[1], **Roopa Dalal**[1], **Yang Sun**[1], **Michael S. Kapiloff**[1], **Jeffrey L. Goldberg**[1], **Wendy W. Liu**[1]

[1]Spencer Center for Vision Research, Byers Eye Institute, Stanford University School of Medicine, Palo Alto, CA, USA

Abstract

PIEZO1 and PIEZO2 are mechanosensitive ion channels that regulate many important physiological processes including vascular blood flow, touch, and proprioception. As the eye is subject to mechanical stress and is highly perfused, these channels may play important roles in ocular function and intraocular pressure regulation. PIEZO channel expression in the eye has not been well defined, in part due to difficulties in validating available antibodies against PIEZO1 and PIEZO2 in ocular tissues. It is also unclear if PIEZO1 and PIEZO2 are differentially expressed. To address these questions, we used single-molecule fluorescence in situ hybridization (smFISH) together with transgenic reporter mice expressing PIEZO fusion proteins under the control of their endogenous promoters to compare the expression and localization of PIEZO1 and PIEZO2 in mouse ocular tissues relevant to glaucoma. We detected both PIEZO1 and PIEZO2 expression in the trabecular meshwork, ciliary body, and in the ganglion cell layer (GCL) of the retina. *Piezo1* mRNA was more abundantly expressed than *Piezo2* mRNA in these ocular tissues. *Piezo1* but not *Piezo2* mRNA was detected in the inner nuclear layer and outer nuclear layer of the retina. Our results suggest that PIEZO1 and PIEZO2 are differentially expressed and may have distinct roles as mechanosensors in glaucoma-relevant ocular tissues.

Keywords

mechanosensitive ion channels; PIEZO channels; expression in the eye; single-molecule fluorescent in situ hybridization; immunohistochemistry; glaucoma

The eye is constantly subjected to mechanical forces induced by normal activities, such as blinking, eye rubbing and eye movements. These activities can cause compression of the eye and drastic fluctuations in intraocular pressure (IOP) (Coleman and Trokel, 1969).

Corresponding author: Wendy W. Liu MD, PhD, Spencer Center for Vision Research, 2370 Watson Court, Palo Alto, CA 94303, Phone: (650) 736-1284, Fax: (650) 565-8297, wendywliu@stanford.edu.

Author Contributions

WWL designed research; YZ, JGS, RD and WWL performed experiments; YZ and WWL analyzed data; YS, MSK and JLG contributed to data interpretation; MSK, JLG and WWL supervised the project; WWL wrote the manuscript, which was approved by the all the authors.

Publisher's Disclaimer: This is a PDF file of an unedited manuscript that has been accepted for publication. As a service to our customers we are providing this early version of the manuscript. The manuscript will undergo copyediting, typesetting, and review of the resulting proof before it is published in its final form. Please note that during the production process errors may be discovered which could affect the content, and all legal disclaimers that apply to the journal pertain.

Author Manuscript Author Manuscript Author Manuscript Author Manuscript

Chronic IOP elevation can cause glaucoma, which is characterized by the loss of retinal ganglion cells (RGCs). How the eye responds and adapts to these mechanical forces is not fully understood. Mechanosensitive ion channels are key pressure sensors that mediate cellular responses to mechanical signals (Arnadóttir and Chalfie, 2010), may play a role in IOP regulation and the development of glaucoma. The recently discovered PIEZO family of mechanosensitive channels, PIEZO1 and PIEZO2, are widely expressed and regulate a wide range of physiological functions, including cardiovascular mechanotransduction (Li et al., 2014; Ranade et al., 2014a), red blood cell volume (Cahalan et al., 2015), light touch (Ranade et al., 2014b), and proprioception (Woo et al., 2015). We have recently reported on genetic variants in *PIEZO1* and *PIEZO2* that show associations with primary open angle glaucoma (Liu et al., 2023). Other studies have implicated roles for PIEZO1 and PIEZO2 in the aqueous outflow pathway (Fang et al., 2021; Morozumi et al., 2021; Yarishkin et al., 2021; Zhu et al., 2021). As members of the same channel family, PIEZO1 and PIEZO2 may have similar or distinct roles in different ocular tissues. However, their expression and function in the eye, as well as their relevance to glaucoma remain largely unknown. Multiple groups have reported that custom-made and commercially available antibodies were not sensitive and specific enough to detect PIEZO expression in a variety of tissues, posing challenges to studying the endogenous expression of these proteins (Acheta et al., 2022; Coste et al., 2010; Dalghi et al., 2019; Li et al., 2021; Ranade et al., 2014a; Yu et al., 2022). Moreover, it is unclear if PIEZO1 and PIEZO2 have similar or unique expression patterns in the eye. In this study, we use single-molecule fluorescence in situ hybridization (smFISH) together with transgenic reporter mice to compare the expression and localization of PIEZO1 and PIEZO2 in the mouse trabecular meshwork, ciliary body, and retina, and discuss their potential roles in the eye and in glaucoma.

All animal research was conducted in compliance with ARVO statement for the use of animals in ophthalmic and vision research and was approved by Institutional Animal Care and Use Committee at Stanford University. Homozygous *Piezo1*^{tdTomato} (B6;129-Piezo1tm1.1Apat/J; Jackson Laboratory #029214) and *Piezo2*^{GFP} (B6(SJL)-Piezo2tm1.1(cre)Apat/J; Jackson Laboratory #027719) mice were as previously described (Ranade et al., 2014a; Woo et al., 2014). C57BL/6 wildtype (WT) mice were obtained from Charles River. Both male and female mice were studied at 6–10 weeks of age.

After euthanasia, eyeballs were immediately removed, embedded in optimal cutting temperature compound (OCT), and flash-frozen in liquid nitrogen. 20 μm cyrosections were used for all experiments. mRNA detection was performed according the manufacturer's protocol for RNAscope Multiplex Fluorescent Reagent Kit V2 (ACDBio) for fresh-frozen tissue. Protease IV was applied for 22 min. Probes (ACDBio) were for mouse *Piezo1* (C1; 400181), mouse *Piezo2* (C2; 400191-C2), mouse *Rbpms* (C3; 527231-C3) and a negative control probe (*Dabp*). *Piezo1* and *Piezo2* probes have been validated previously (Fernández-Trillo et al., 2020; Hill et al., 2022; Ma et al., 2021; Marshall et al., 2020). Quantification of the target probes and negative control probe was performed using QuPath (Bankhead et al., 2017). After using regions of interest (ROIs) to define the quantification area, cell segmentation was performed based on DAPI nuclear signal using the "Cell Detection" function, and the "Subcellular Detection" function was used to calculate the number of transcripts for each probe. Cells with ≥ 1 transcript were considered positive for expression,

Author Manuscript Author Manuscript Author Manuscript Author Manuscript

based on the negative control probe. At least 3 biological replicates were analyzed. One way ANOVAs with Tukey's post hoc tests were used to compare the percentage of cells positive for *Piezo1*, *Piezo2*, or both.

Several protocols for immunohistochemistry (IHC) were attempted and a modified protocol was found to provide the highest signal-to-noise ratio, as follows (Dalghi et al., 2019; Hill et al., 2022). The sections were rinsed with PBS to remove OCT and subsequently post-fixed with 4% paraformaldehyde (PFA) in PBS for 10 minutes at room temperature. The sections were then quenched using a solution of PBS containing 20 mM glycine, 75 mM ammonium chloride, and 0.1% Triton X-100 for 10 minutes. The slides were washed with PBS for 3–5 times to remove any residual fixative. To block non-specific binding, the sections were incubated with blocking buffer (PBS with 0.6% fish skin gelatin, 0.05% saponin, and 5% normal goat serum) for 1 hour at room temperature. Primary antibodies were applied overnight at 4°C in blocking buffer without serum: 1:200 rabbit anti-RFP (Rockland 600–401-379), 1:500 chicken anti-GFP (Abcam ab13970), 1:500 rat anti-PECAM-1 (BD Pharming 553370), 1:1000 guinea pig anti-RBPMS (made in-house), and 1:200 mouse anti-alpha smooth muscle actin (Abcam ab7817). The sections were washed with PBS for 3–5 times before incubation with secondary antibodies in blocking buffer without serum for 1 hour at room temperature. All secondary antibodies were used at a dilution of 1:1000: goat anti-rabbit AlexaFluor 555 (Life Technologies A21429), goat anti-guinea pig AlexaFluor 488 (Life Technologies A11073), goat anti-mouse AlexaFluor 488 (Life Technologies A11029), goat anti-chicken AlexaFluor 555 (Life Technologies A32932), goat anti-rat AlexaFluor 647 (Life Technologies A21247). After washing the sections with PBS, samples were mounted with SlowFade Diamond and sealed with nail polish. Samples were imaged on an Olympus confocal microscope using matched settings. For all images, brightness and contrast adjustments were applied uniformly across the entire image. At least three biological replicates were performed for each experiment. After defining ROIs, mean fluorescent intensities were measured using Fiji. Paired t tests were used to compare the signal intensities between PIEZO reporter mice and matched WT controls.

Previous studies have reported that PIEZO antibodies lack sufficient sensitivity and specificity for reliable immunohistochemistry (Acheta et al., 2022; Coste et al., 2010; Dalghi et al., 2019; Li et al., 2021; Ranade et al., 2014a; Yu et al., 2022). As we too found it difficult to detect endogenous PIEZO1 and PIEZO2 in tissue using antibodies against PIEZO, we used both single-molecule fluorescence in situ hybridization (smFISH) and *Piezo1*^{tdTomato} and *Piezo2*^{GFP} knock-in reporter mice to define the expression of PIEZO1 and PIEZO2 mRNA and protein in ocular tissues. *Piezo1*^{tdTomato} and *Piezo2*^{GFP} express tdTomato and Green Fluorescent Protein (EGFP) C-terminal fusion proteins of PIEZO1 and PIEZO2, respectively, under the control of their native promoters (Woo et al., 2014). PIEZO fusion proteins were detected using antibodies for the fluorescent protein tags. We focused on detecting PIEZO expression in in the trabecular meshwork, ciliary body, and the retina, as these tissues play a role in IOP regulation and glaucomatous neurodegeneration. We sought to determine if there were differences in PIEZO1 and PIEZO2 expression in these ocular tissues relevant to glaucoma.

Author Manuscript Author Manuscript Author Manuscript Author Manuscript

We observed both *Piezo1* and *Piezo2* mRNA in the trabecular meshwork (Fig 1A). *Piezo1* mRNA was more abundant, with 41.2 ± 5.1% of cells expressing *Piezo1* versus 15.3 ± 7.6% expressing *Piezo2* ($P<0.01$). 9.7 ± 2.6% expressed both *Piezo1* and *Piezo2* (Fig 1B). Using IHC to detect PIEZO fusion proteins, we could not detect significant PIEZO1^{tdTomato} and PIEZO2^{GFP} staining in the trabecular meshwork above background signal, which was counter-stained with α-smooth muscle actin (Fig 1C, 1D, 1E, 1F).

In the ciliary body, we observed robust expression of both *Piezo1* mRNA (Fig 1G), with 72.1 ± 8.4% of cells positive for *Piezo1* (Fig 1H). Significantly fewer cells expressed *Piezo2* mRNA (1.8 ± 3.2%) ($P<0.0001$), and most cells expressing *Piezo2* also expressed *Piezo1* (1H). By IHC, we detected tdTomato fusion protein in the ciliary body epithelium (Fig 1I, 1J) but there was no detectable PIEZO2^{GFP} expression (Fig 1K, 1L).

In the retina, smFISH showed *Piezo1* mRNA in the ganglion cell layer (GCL) and inner nuclear layer (INL), and a low level of *Piezo1* mRNA in the outer nuclear layer (ONL) (Fig 2A). Some *Piezo1* mRNA in the GCL was present in retinal ganglion cells (RGCs) detected by *Rbpms* transcript (Fig 2B). *Piezo1* was expressed in 39.0 ± 13.4% of cells in in the GCL, 40.0% ± 7.6% in the INL, and 14.6% ± 3.6% in the ONL (Fig 2C). Significantly fewer cells expressed *Piezo2* mRNA in the GCL (6.1 ± 8.7%) ($P<0.0001$) (Fig 2A, 2C), and most of these *Piezo2*-positive cells also expressed *Piezo1*. *Piezo2* mRNA was not detected in the INL and ONL (Fig 2A, 2C). By IHC, PIEZO1^{tdTomato} signal co-localized with PECAM-1, a marker for blood vessels, in the retinal capillary plexuses (Fig 2D). We also found faint PIEZO1^{tdTomato} signal that co-localized with some RBPMS-positive cells, suggesting PIEZO1^{tdTomato} expression in a subset of RGCs (Fig 2E). However, mean PIEZO1^{tdTomato} signal across the GCL was not significantly elevated over background (Fig 2F). There was no detectable PIEZO1^{tdTomato} expression in the INL or ONL (Fig 2D, 2F). PIEZO2^{GFP} was also not detected in the GCL, INL or ONL (Fig 2G, 2H, 2I).

Although PIEZO1 and PIEZO2 play diverse physiological roles in many organ systems (Syeda, 2021), the expression and role of PIEZO1 and PIEZO2 in the eye and their relevance to glaucoma have been less studied. Genetic variants of *PIEZO1* and *PIEZO2* have been implicated in glaucoma (Liu et al., 2023), but it is unknown if PIEZO1 and PIEZO2 play similar or distinct roles in ocular tissues. In this study, we compare PIEZO1 and PIEZO2 expression in the trabecular meshwork, ciliary body, and retina using smFISH and reporter mice that label PIEZO1 and PIEZO2 expressed from their endogenous promoters.

Our work highlights the challenges to detecting endogenous PIEZO expression, due in part to the low level of PIEZO expression in many cell types. The expression of PIEZO1 and PIEZO2 in some tissues of the eye were described previously using commercially available antibodies (Fang et al., 2021; Fernández-Trillo et al., 2020; Morozumi et al., 2021; Yarishkin et al., 2021; Zhu et al., 2021). Due to difficulties with confirming the sensitivity and specificity of commercial antibodies in ocular tissues, we used smFISH and IHC of PIEZO1^{tdTomato} and PIEZO2^{GFP} from reporter mice. For IHC, we used matched control wild-type mice processed under the same conditions to control for varying background signals in different ocular tissues. Nonetheless, it is possible that our methods are insufficiently sensitive to detect low, but functionally relevant levels of channel

Author Manuscript Author Manuscript Author Manuscript Author Manuscript

expression. In the trabecular meshwork and parts of the retina, we could detect *Piezo* mRNA by smFISH, but not PIEZO reporter protein expression. smFISH provides high sensitivity and resolution in detecting RNA individual molecules. Our use of reporter mice with IHC provides complementary information about expression at the protein level. However, PIEZO protein expression may be too low to detect even after amplifying the signal with antibodies against the fluorescent reporter, as reported previously (Dalghi et al., 2019). As PIEZO channels are membrane proteins, total internal reflection microscopy may be useful in certain applications (Holt et al., 2021; Jairaman et al., 2021).

Mechanotransduction via PIEZO1 and PIEZO2 in the trabecular meshwork and iridocorneal angle tissues have been suggested to regulate aqueous humor outflow and IOP (Fang et al., 2021; Morozumi et al., 2021; Yarishkin et al., 2021; Zhu et al., 2021). We detected *Piezo1* and *Piezo2* mRNA in the trabecular meshwork, suggesting that both PIEZO1 and PIEZO2 may contribute to trabecular meshwork function and IOP regulation. However, both endogenous PIEZO1 and PIEZO2 protein expression were too low to be detected via IHC in PIEZO reporter mice. In the ciliary body process, PIEZO1 and PIEZO2 showed distinct expression patterns. There was robust expression of PIEZO1 protein and mRNA in the ciliary body epithelium but only rare *Piezo2* mRNA, suggesting a more dominant role for PIEZO1 in aqueous humor production. While other ion channels such as chloride channels are known to modulate aqueous humor formation (Do and Civan, 2006), the role of PIEZO1 in the ciliary body has not been described. Future work is warranted to determine how PIEZO channels may regulate both aqueous humor inflow and outflow, and how they may play a role in IOP modulation and glaucoma.

In the retina, the expression patterns of PIEZO1 and PIEZO2 were again distinct. PIEZO1 was prominently expressed in retinal blood vessels, consistent with their established role in vascular development (Li et al., 2014; Ranade et al., 2014a). In addition, we detected *Piezo1* mRNA in the GCL and INL, and at a low level in the ONL, suggesting a role in retinal neurons. Some RGCs also express PIEZO1. A low level of *Piezo2* mRNA was found in the GCL. A previous in vitro study suggested that PIEZO1 affects neurite outgrowth in RGCs (Morozumi et al., 2020). It remains to be seen whether PIEZO channels affect neuronal physiology or visual processing, and whether they mediate responses to IOP.

Our results show that PIEZO1 and PIEZO2 are co-expressed in some ocular tissues (e.g. trabecular meshwork), while PIEZO1 is singly expressed in others (e.g. INL and ONL). While both *Piezo1* and *Piezo2* mRNA are expressed in the trabecular meshwork, ciliary body, and GCL, *Piezo1* is expressed more abundantly than *Piezo2*. Many tissues, including bladder, colon and lung express both PIEZO1 and PIEZO2 (Coste et al., 2010). Although much is still unknown regarding how these channels are physiologically activated and the associated mechanotransduction pathways they govern, evidence suggests that PIEZO1 and PIEZO2 can have synergistic or distinct functional roles (Dalghi et al., 2019). Previous studies of PIEZO channels and aqueous humor outflow have only focused on either PIEZO1 or PIEZO2 (Fang et al., 2021; Morozumi et al., 2021; Yarishkin et al., 2021; Zhu et al., 2021). Future studies of both PIEZO1 and PIEZO2 in the same ocular tissues would be invaluable for determining whether these channels serve similar or divergent roles.

Author Manuscript Author Manuscript Author Manuscript Author Manuscript

Our results are consistent with published single-cell RNA sequencing data showing that PIEZO1 and PIEZO2 are expressed at low levels in many cell types in the human trabecular meshwork, ciliary body and retina (Peng et al., 2019; van Zyl et al., 2020; van Zyl et al., 2022). Our ISH and IHC results offer a complementary approach to understanding the localization and expression of PIEZO channels in the eye, and provide new insights into the differential expression of PIEZO1 and PIEZO2 in different ocular tissues. Further work is needed to characterize the diverse aspects of PIEZO channel function in ocular physiology and pathology, as well as their relevance to glaucoma.

Acknowledgements

Support was provided by NIH grants KL2TR003143 (WWL), K08EY034600 (WWL), R01-EY031167 (MSK), R01-EY032416 (MSK & JLG), R01-EY025295 (Y.S.), VA merit CX001298 (Y.S), the American Glaucoma Society (WWL), a Research to Prevent Blindness Career Development Award (WWL), the Glaucoma Research Foundation (WWL), the E. Matilda Ziegler Foundation for the Blind (WWL), the NIH NEI P30 Vision Research Core (EY026877, Stanford Ophthalmology), and an unrestricted grant from Research to Prevent Blindness (Stanford Ophthalmology).

References

Acheta J, Bhatia U, Haley J, Hong J, Rich K, Close R, Bechler ME, Belin S, Poitelon Y, 2022. Piezo channels contribute to the regulation of myelination in Schwann cells. Glia 70, 2276–2289. [PubMed: 35903933]

Arnadóttir J, Chalfie M, 2010. Eukaryotic mechanosensitive channels. Annu Rev Biophys 39, 111–137. [PubMed: 20192782]

Bankhead P, Loughrey MB, Fernández JA, Dombrowski Y, McArt DG, Dunne PD, McQuaid S, Gray RT, Murray LJ, Coleman HG, James JA, Salto-Tellez M, Hamilton PW, 2017. QuPath: Open source software for digital pathology image analysis. Scientific Reports 7.

Cahalan SM, Lukacs V, Ranade SS, Chien S, Bandell M, Patapoutian A, 2015. Piezo1 links mechanical forces to red blood cell volume. Elife 4.

Coleman DJ, Trokel S, 1969. Direct-recorded intraocular pressure variations in a human subject. Arch Ophthalmol 82, 637–640. [PubMed: 5357713]

Coste B, Mathur J, Schmidt M, Earley TJ, Ranade S, Petrus MJ, Dubin AE, Patapoutian A, 2010. Piezo1 and Piezo2 are essential components of distinct mechanically activated cation channels. Science 330, 55–60. [PubMed: 20813920]

Dalghi MG, Clayton DR, Ruiz WG, Al-Bataineh MM, Satlin LM, Kleyman TR, Ricke WA, Carattino MD, Apodaca G, 2019. Expression and distribution of PIEZO1 in the mouse urinary tract. American journal of physiology. Renal physiology 317, F303–F321. [PubMed: 31166705]

Do CW, Civan MM, 2006. Swelling-activated chloride channels in aqueous humour formation: on the one side and the other. Acta Physiologica 187, 345–352. [PubMed: 16734771]

Fang J, Hou F, Wu S, Liu Y, Wang L, Zhang J, Wang N, Wang K, Zhu W, 2021. Piezo2 downregulation via the Cre-lox system affects aqueous humor dynamics in mice. Molecular vision 27, 354–364. [PubMed: 34220183]

Fernández-Trillo J, Florez-Paz D, Íñigo-Portugués A, González-González O, del Campo AG, González A, Viana F, Belmonte C, Gomis A, 2020. Piezo2 Mediates Low-Threshold Mechanically Evoked Pain in the Cornea. The Journal of Neuroscience 40, 8976–8993. [PubMed: 33055278]

Hill RZ, Loud MC, Dubin AE, Peet B, Patapoutian A, 2022. PIEZO1 transduces mechanical itch in mice. Nature 607, 104–110. [PubMed: 35732741]

Holt JR, Zeng W-Z, Evans EL, Woo S-H, Ma S, Abuwarda H, Loud M, Patapoutian A, Pathak MM, 2021. Spatiotemporal dynamics of PIEZO1 localization controls keratinocyte migration during wound healing. eLife 10, e65415. [PubMed: 34569935]

Author Manuscript Author Manuscript Author Manuscript Author Manuscript

Jairaman A, Othy S, Dynes JL, Yeromin AV, Zavala A, Greenberg ML, Nourse JL, Holt JR, Cahalan SM, Marangoni F, Parker I, Pathak MM, Cahalan MD, 2021. Piezo1 channels restrain regulatory T cells but are dispensable for effector CD4(+) T cell responses. Sci Adv 7.

Li J, Hou B, Tumova S, Muraki K, Bruns A, Ludlow MJ, Sedo A, Hyman AJ, McKeown L, Young RS, Yuldasheva NY, Majeed Y, Wilson LA, Rode B, Bailey MA, Kim HR, Fu Z, Carter DA, Bilton J, Imrie H, Ajuh P, Dear TN, Cubbon RM, Kearney MT, Prasad RK, Evans PC, Ainscough JF, Beech DJ, 2014. Piezo1 integration of vascular architecture with physiological force. Nature 515, 279–282. [PubMed: 25119035]

Li J, Liu S, Song C, Hu Q, Zhao Z, Deng T, Wang Y, Zhu T, Zou L, Wang S, Chen J, Liu L, Hou H, Yuan K, Zheng H, Liu Z, Chen X, Sun W, Xiao B, Xiong W, 2021. PIEZO2 mediates ultrasonic hearing via cochlear outer hair cells in mice. Proceedings of the National Academy of Sciences 118, e2101207118.

Liu WW, Kinzy TG, Cooke Bailey JN, Xu Z, Hysi P, Wiggs JL, 2023. Mechanosensitive ion channel gene survey suggests potential roles in primary open angle glaucoma. Sci Rep 13, 15871. [PubMed: 37741866]

Ma S, Dubin AE, Zhang Y, Mousavi SAR, Wang Y, Coombs AM, Loud M, Andolfo I, Patapoutian A, 2021. A role of PIEZO1 in iron metabolism in mice and humans. Cell 184, 969–982.e913. [PubMed: 33571427]

Marshall KL, Saade D, Ghitani N, Coombs AM, Szczot M, Keller J, Ogata T, Daou I, Stowers LT, Bönnemann CG, Chesler AT, Patapoutian A, 2020. PIEZO2 in sensory neurons and urothelial cells coordinates urination. Nature 588, 290–295. [PubMed: 33057202]

Morozumi W, Aoshima K, Inagaki S, Iwata Y, Nakamura S, Hara H, Shimazawa M, 2021. Piezo 1 is involved in intraocular pressure regulation. Journal of Pharmacological Sciences 147, 211–221. [PubMed: 34217619]

Morozumi W, Inagaki S, Iwata Y, Nakamura S, Hara H, Shimazawa M, 2020. Piezo channel plays a part in retinal ganglion cell damage. Exp Eye Res 191, 107900. [PubMed: 31874142]

Peng YR, Shekhar K, Yan W, Herrmann D, Sappington A, Bryman GS, van Zyl T, Do MTH, Regev A, Sanes JR, 2019. Molecular Classification and Comparative Taxonomics of Foveal and Peripheral Cells in Primate Retina. Cell 176, 1222–1237.e1222. [PubMed: 30712875]

Ranade SS, Qiu Z, Woo SH, Hur SS, Murthy SE, Cahalan SM, Xu J, Mathur J, Bandell M, Coste B, Li YS, Chien S, Patapoutian A, 2014a. Piezo1, a mechanically activated ion channel, is required for vascular development in mice. Proc Natl Acad Sci U S A 111, 10347–10352. [PubMed: 24958852]

Ranade SS, Woo S-H, Dubin AE, Moshourab RA, Wetzel C, Petrus M, Mathur J, Bégay V, Coste B, Mainquist J, Wilson AJ, Francisco AG, Reddy K, Qiu Z, Wood JN, Lewin GR, Patapoutian A, 2014b. Piezo2 is the major transducer of mechanical forces for touch sensation in mice. Nature 516, 121–125. [PubMed: 25471886]

Syeda R, 2021. Physiology and Pathophysiology of Mechanically Activated PIEZO Channels. Annu Rev Neurosci 44, 383–402. [PubMed: 34236889]

van Zyl T, Yan W, McAdams A, Peng Y-R, Shekhar K, Regev A, Juric D, Sanes JR, 2020. Cell atlas of aqueous humor outflow pathways in eyes of humans and four model species provides insight into glaucoma pathogenesis. Proceedings of the National Academy of Sciences 117, 10339–10349.

van Zyl T, Yan W, McAdams AM, Monavarfeshani A, Hageman GS, Sanes JR, 2022. Cell atlas of the human ocular anterior segment: Tissue-specific and shared cell types. Proc Natl Acad Sci U S A 119, e2200914119. [PubMed: 35858321]

Woo SH, Lukacs V, de Nooij JC, Zaytseva D, Criddle CR, Francisco A, Jessell TM, Wilkinson KA, Patapoutian A, 2015. Piezo2 is the principal mechanotransduction channel for proprioception. Nature neuroscience 18, 1756–1762. [PubMed: 26551544]

Woo SH, Ranade S, Weyer AD, Dubin AE, Baba Y, Qiu Z, Petrus M, Miyamoto T, Reddy K, Lumpkin EA, Stucky CL, Patapoutian A, 2014. Piezo2 is required for Merkel-cell mechanotransduction. Nature 509, 622–626. [PubMed: 24717433]

Yarishkin O, Phuong TTT, Baumann JM, De Ieso ML, Vazquez-Chona F, Rudzitis CN, Sundberg C, Lakk M, Stamer WD, Križaj D, 2021. Piezo1 channels mediate trabecular meshwork

Author Manuscript Author Manuscript Author Manuscript Author Manuscript

mechanotransduction and promote aqueous fluid outflow. J Physiol 599, 571–592. [PubMed: 33226641]

Yu Z-Y, Gong H, Kesteven S, Guo Y, Wu J, Li JV, Cheng D, Zhou Z, Iismaa SE, Kaidonis X, Graham RM, Cox CD, Feneley MP, Martinac B, 2022. Piezo1 is the cardiac mechanosensor that initiates the cardiomyocyte hypertrophic response to pressure overload in adult mice. Nature Cardiovascular Research 1, 577–591.

Zhu W, Hou F, Fang J, Bahrani Fard MR, Liu Y, Ren S, Wu S, Qi Y, Sui S, Read AT, Sherwood JM, Zou W, Yu H, Zhang J, Overby DR, Wang N, Ethier CR, Wang K, 2021. The role of Piezo1 in conventional aqueous humor outflow dynamics. iScience 24, 102042. [PubMed: 33532718]

Author Manuscript Author Manuscript Author Manuscript Author Manuscript

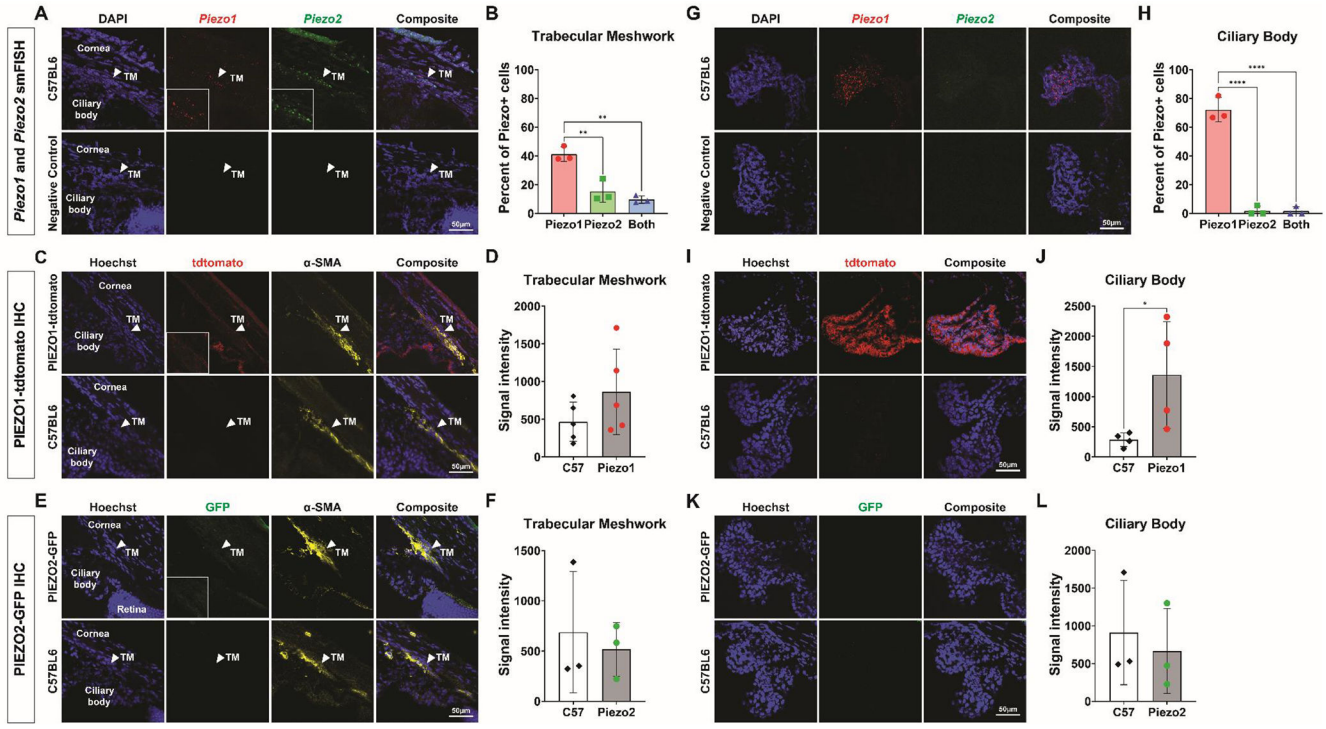

Figure 1.

PIEZO expression in the trabecular meshwork and ciliary body. (A) smFISH for *Piezo1*, *Piezo2* with DAPI (top), and for a negative control probe (bottom) in a sectioned C57BL6 wild-type mouse eye. Arrowhead indicates the trabecular meshwork (TM). Inset shows region around arrowhead magnified 3.2x. (B) Quantification of smFISH images comparing the percentage of cells expressing *Piezo1* or *Piezo2*, or both in the trabecular meshwork using one-way ANOVA. (C) IHC of sectioned PIEZO1^{tdTomato} (top) and C57BL6 wild-type (bottom) mouse eye labeled with antibodies against tdTomato, alpha-smooth muscle actin (α-SMA), and Hoescht. Arrowhead indicates the trabecular meshwork. Inset shows region around arrowhead magnified 3.2x. (D) Quantification of IHC images comparing the mean fluorescent signal intensities between PIEZO1^{tdTomato} samples and C57BL6 wild-type samples in the trabecular meshwork using paired t test. (E) IHC of sectioned PIEZO2^{GFP} (top) and C57BL6 wild-type (bottom) mouse eye labeled with antibodies against GFP, α-SMA, and Hoescht. Arrowhead indicates the trabecular meshwork. Inset shows region around arrowhead magnified 3.2x. (F) Quantification of IHC images comparing the mean fluorescent signal intensities between PIEZO2^{GFP} samples and C57BL6 wild-type samples in the trabecular meshwork using paired t test. (G) smFISH for with *Piezo1*, *Piezo2* with DAPI (top), and for a negative control probe (bottom) in a sectioned C57BL6 wild-type mouse eye. (H) Quantification of smFISH images comparing the percentage of cells expressing *Piezo1* or *Piezo2*, or both in the ciliary body using one-way ANOVA. (I) IHC of sectioned PIEZO1^{tdTomato} (top) and C57BL6 wild-type (bottom) mouse eye labeled with antibodies against tdTomato and Hoescht. (J) Quantification of IHC images comparing the mean fluorescent signal intensities between PIEZO1^{tdTomato} samples and C57BL6 wild-type samples in the ciliary body using paired t test. (K) IHC of sectioned PIEZO2^{GFP} (top) and C57BL6 wild-type (bottom) mouse eye labeled with antibodies against GFP and Hoescht.

Author Manuscript Author Manuscript Author Manuscript Author Manuscript

(L) Quantification of IHC images comparing the mean fluorescent signal intensities between PIEZO2^{GFP} samples and C57BL6 wild-type samples in the ciliary body using paired t test. *P<0.05. **P<0.01. ****P<0.0001. smFISH, single-molecule fluorescence in situ hybridization. IHC, immunohistochemistry. TM, trabecular meshwork.

Author Manuscript Author Manuscript Author Manuscript Author Manuscript

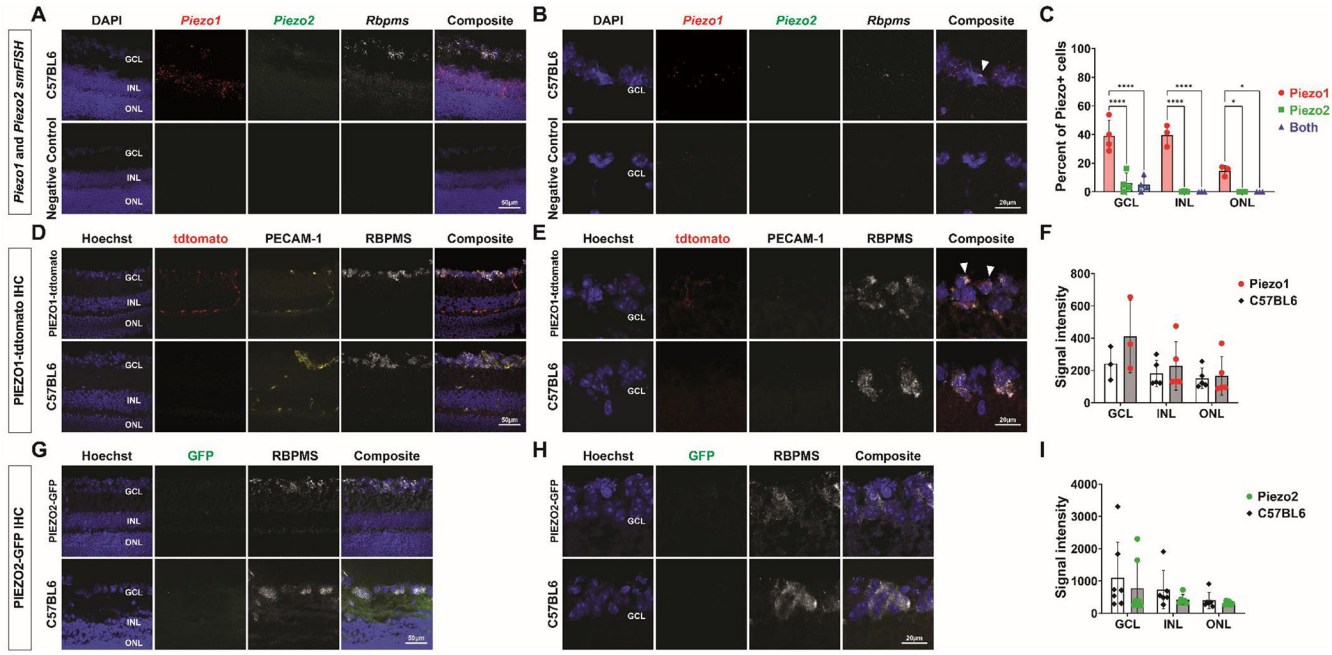

Figure 2.

PIEZO expression in the retina. (A) smFISH for with *Piezo1*, *Piezo2*, *Rbpms*, with DAPI (top), and for a negative control probe (bottom) in a sectioned C57BL6 wild-type mouse eye. (B) Higher magnification smFISH images of the ganglion cell layer (GCL) shows *Piezo1* transcript localizing in some *Rbpms*$^{+}$ cells (top, arrowhead). Higher magnification images for a negative control probe are shown below. (C) Quantification of smFISH images comparing the percentage of cells expressing *Piezo1* or *Piezo2*, or both in the GCL, INL, and ONL using one-way ANOVAs. (D) IHC of sectioned PIEZO1^{tdTomato} (top) and C57BL6 wild-type (bottom) mouse eye labeled with antibodies against tdTomato, RBPMS, PECAM-1, and Hoescht. (E) Higher magnification IHC images of the ganglion cell layer (GCL) from PIEZO1^{tdTomato} sections shows PIEZO1^{tdTomato} signal co-localizing with RBPMS and not PECAM-1 (top, arrowheads). Higher magnification images from C57BL6 sections are shown below. (F) Quantification of IHC images comparing the mean fluorescent signal intensities between PIEZO1^{tdTomato} samples and C57BL6 wild-type samples in the GCL, INL, and ONL using paired t tests. (G) IHC of sectioned PIEZO2^{GFP} (top) and C57BL6 wild-type (bottom) mouse eye labeled with antibodies against GFP, RBPMS, and Hoescht. (H) Higher magnification IHC images of the ganglion cell layer (GCL) from PIEZO2^{GFP} sections shows no detectable PIEZO2^{GFP} signal (top). Higher magnification images from C57BL6 sections are shown below. (I) Quantification of IHC images comparing the mean fluorescent signal intensities between PIEZO2^{GFP} samples and C57BL6 wild-type samples in the GCL, INL, and ONL using paired t tests *P<0.05. ****P<0.0001. smFISH, single-molecule fluorescence in situ hybridization. IHC, immunohistochemistry. GCL, ganglion cell layer. INL, inner nuclear layer. ONL, outer nuclear layer.